

This is the accepted manuscript version of the contribution published as:

Phillips, E., Bulka, O., Picott, K., **Kümmel, S.**, Edwards, E., **Nijenhuis, I.**, **Gehre, M.**, Dworatzek, S., Webb, J., Sherwood Lollar, B. (2022):
Investigation of active site amino acid influence on carbon and chlorine isotope fractionation during reductive dechlorination
FEMS Microbiol. Ecol. **98** (8), fiac072

The publisher's version is available at:

<http://dx.doi.org/10.1093/femsec/fiac072>

Investigation of Active Site Amino Acid Influence on Carbon and Chlorine Isotope Fractionation during Reductive Dechlorination

Elizabeth Phillips[†], *Olivia Bulka*[§], *Katherine Picott*[§], *Steffen Kümmel*[‡], *Elizabeth Edwards*[§],
Ivonne Nijenhuis[‡], *Matthias Gehre*[‡], *Sandra Dworatzek*[⊥], *Jennifer Webb*[⊥], *Barbara Sherwood Lollar*^{†*}

[†] Department of Earth Sciences, University of Toronto, 22 Ursula Franklin Street, Toronto, Ontario M5S 3B1, Canada

[§] Department of Chemical Engineering and Applied Chemistry, University of Toronto, 200 College Street, Toronto, Ontario M5S 3E5, Canada

[‡] Department of Isotope Biogeochemistry, Helmholtz Centre for Environmental Research – UFZ, Permoserstrasse 15, 04318 Leipzig, Germany

[⊥] SiREM, Guelph, ON, N1G 3Z2, Canada

***Corresponding author**

Barbara Sherwood Lollar

University of Toronto

Department of Earth Sciences

22 Ursula Franklin St.

Toronto, ON M5S 3B1, Canada

Phone: (416) 978-0770

Fax: (416) 978-3938

E-mail: barbara.sherwoodlollar@utoronto.ca

Abstract

Reductive dehalogenases (RDases) are corrinoid-dependent enzymes that reductively dehalogenate organohalides in respiratory processes. By comparing isotope effects in biotically-catalyzed reactions to reference experiments with abiotic corrinoid-catalysts, compound-specific isotope analysis (CSIA) has been shown to yield valuable insights into enzyme mechanisms and kinetics, including RDases. Here, we report isotopic fractionation (ϵ) during biotransformation of chloroform (CF) for carbon ($\epsilon_C = -1.52 \pm 0.34\text{‰}$) and chlorine ($\epsilon_{Cl} = -1.84 \pm 0.19\text{‰}$), corresponding to a $\Lambda_{C/Cl}$ value of 1.13 ± 0.35 . These results are highly suppressed compared to isotope effects observed both during CF biotransformation by another organism with a highly similar RDase (> 95% sequence identity) at the amino acid level, and to those observed during abiotic dehalogenation of CF. Amino acid differences occur at four locations within the two different RDases' active sites, and this study examines whether these differences potentially affect the observed ϵ_C , ϵ_{Cl} , and $\Lambda_{C/Cl}$. Structural protein models approximating the locations of the residues elucidate possible controls on reaction mechanisms and/or substrate binding efficiency. These four locations are not conserved among other chloroalkane reducing RDases with high

amino acid similarity (> 90%), suggesting that these locations may be important in determining isotope fractionation within this homologous group of RDases.

Keywords: Compound-specific isotope analysis, amino acid identity, reductive dehalogenases, biotransformation, chlorinated alkanes, reductive dechlorination

Introduction

Halogenated alkanes are aliphatic compounds that include chlorinated methanes such as chloroform (CF) and dichloromethane (DCM), and chlorinated ethanes such as 1,1,1-trichloroethane (1,1,1-TCA) and 1,1-dichloroethane (1,1-DCA). These compounds are common groundwater contaminants at many sites due to past spills or poor storage and disposal practices (Fent, 2003; Rowe et al., 2007). As the threats of halogenated alkanes to human and environmental health have become more understood, organizations such as Health Canada (Health Canada, 2020), the U.S. Environmental Protection Agency (USEPA) (USEPA, 2012), and the World Health Organization (WHO) (WHO, 2004) have introduced regulations and recommendations for maximum concentrations in groundwater on the order of parts per billion (ppb). As a result, research on transformation mechanisms and pathways of these compounds has proliferated in the past 50 years to inform remediation strategies.

Organohalide-respiring bacteria (OHRB) are a diverse group of microbes that transform organohalides via reductive dehalogenation as part of their metabolism (Adrian and Löffler, 2016). These organisms use enzymes called reductive dehalogenases (referred to as RDases when functionally characterized, or RdhA when uncharacterized but predicted from genomes;

Adrian and Löffler, 2016), a class of corrinoid-dependent terminal reductases in organohalide respiration (Adrian and Löffler, 2016). RDases generally transform organohalides, most commonly organochlorides, by removing one or more chlorine atom(s), via pathways such as hydrogenolysis or reductive elimination (e.g., β -elimination). Applying OHRB for organohalide remediation in groundwater has garnered a high level of interest, but considerable knowledge gaps persist, including details of specific reaction mechanisms, substrate specificity, and enzymatic activity. Establishing methods to design and optimize in situ biotransformation strategies based on the substrates and concentrations present at a site (e.g., by identifying if critical native microorganisms are present via genetic characterization) may be enhanced by a better understanding of the relationship between RDase amino acid sequences and function.

RDases are classified into 'ortholog groups' (OGs) based on their amino acid sequence similarity, grouping RDases with at least 90% sequence identity (Hug et al., 2013). In many cases, RDases within OGs have similarities in function, such as biotransformation of the same substrates (Molenda et al., 2020). OG 97 is described as a group of dehalogenases that transform chlorinated alkanes (e.g. 1,1,1-trichloroethane/chloroform/1,1-dichloroethane) (Molenda et al., 2020). Members of this group include characterized proteins ThmA (Zhao et al., 2017), CtrA (Zhao et al., 2015), TmrA (Deshpande et al., 2013; Jugder et al., 2017), CfrA (Tang et al., 2012), and DcrA (Tang et al., 2012). Interestingly, despite the high similarity of these enzymes (> 90% in amino acid identity), each enzyme in OG97 exhibits differences in their substrate ranges and preferences (see Table 1 footnote). For example, the RDase CfrA can dechlorinate 1,1,1-TCA and CF but shows no transformation of 1,1-DCA, while a very similar protein, DcrA, transforms 1,1-DCA, but not CF or 1,1,1-TCA (Tang and Edwards, 2013). Both CfrA and DcrA transform 1,1,2-TCA (Wang et al., 2017). This substrate specificity is observed despite their high similarity

at the amino acid level (95.2%) (Tang and Edwards, 2013). Molenda et al. (2020) found important links between OGs and function (specifically, reductive dechlorination of chlorinated methanes and ethanes by multiple enzymes in OG 97) but noted that future work is required to establish the causal links between reductive dehalogenase amino acid sequence and function.

Typical characteristics of OHRB, such as slow growth rates and sensitivity to oxygen, combined with the scarcity of biochemical tools for purifying RDases through heterologous expression, have challenged biochemical characterization. Recent developments in heterologous expression (Halliwell et al., 2021; Jugder et al., 2018; Mac Nelly et al., 2014; Nakamura et al., 2018; Parthasarathy et al., 2015; Picott et al., 2022) and structural characterization (Bommer et al., 2014; Kunze et al., 2017; Payne et al., 2015) of RDases have been key to overcoming these challenges and further advancing mechanistic and structural characterization. Numerous reaction mechanisms have been proposed, including a direct interaction of the super-reduced cobalt (Co^{I}) of the corrinoid with the substrate; forming a cobalt-carbon bond in a nucleophilic substitution reaction (Schrauzer and Deutsch, 1968), or a cobalt-halogen bond (Payne et al., 2015); and long-range electron transfer from Co^{I} to form a substrate radical intermediate, followed by elimination of the halogen to form a carbanion (Bommer et al., 2014; Kunze et al., 2017; Schmitz et al., 2007; Ye et al., 2010). Electron transfer processes can also be investigated to determine if they involve bond formation between the electron donor and acceptor (inner sphere electron transfer) (Saveant, 1990) or not (outer sphere electron transfer) (Marcus, 1992). To date, studies utilizing heterologous expression and structural characterization have been most successful for RDases from non-obligate OHRB, including mostly chlorinated ethene degrading RDases (e.g. see Molenda et al., 2020). Obligate OHRB (such as *Dehalobacter*) are very sensitive to oxygen, grow much more slowly and yield much less biomass than facultative OHRB (Adrian and

Löffler, 2016), making their enzymes harder to characterize biochemically (e.g. see Fincker and Spormann, 2017). However, recent advances in structural protein modelling (Baek et al., 2021; Jumper et al., 2021) can provide insight into the location of amino acid residues relative to the active site and allow hypothesis generation about their influence on activity and substrate range.

Compound-specific isotope analysis (CSIA) has become an established tool in contaminant hydrogeology to identify and quantitatively estimate the extent of transformation of volatile organic compounds (VOCs) in groundwater (Hunkeler et al., 2008). CSIA also has been applied to probe enzymatic mechanisms and kinetics (recently reviewed by Ojeda et al. (2020); Vogt et al. (2016)). Using CSIA, the stable isotope ratios of an element are measured at natural abundance. CSIA in mechanistic studies is based on the kinetic isotope effect (KIE), where molecules with the same chemical composition but different isotopic composition (isotopologues) generally react slightly faster if they contain exclusively light isotopes of an element (^LE) than if they contain one or more heavy isotopes of an element (^HE) in a reacting bond or its vicinity, corresponding to a normal isotope effect. It should be noted that inverse isotope effects can also be observed (e.g., Heckel et al., 2019) where the heavy isotopologue reacts faster than the light, but these are generally less frequent. Regardless, changing stable isotope ratios (R , where $R = \frac{^H\text{E}}{^L\text{E}}$) in a compound over the course of a chemical reaction is referred to as isotope fractionation.

In first-order reactions, the KIE is equal to the ratio of rate constants for heavy and light isotopologues ($\frac{k^H}{k^L}$) (Bigeleisen, 1949). The intrinsic KIE is related to the order and manner of bond breakage in a chemical reaction and hence can provide insights into reaction mechanisms. However, the observed isotope effect (apparent KIE, AKIE) can be substantially different from the intrinsic KIE due to differences in rate-limiting steps in the net enzymatic reaction.

Biotransformation pathways are typically comprised of multiple elementary reaction steps, including non-transformation steps such as mass transfer (Bosma et al., 1997), or binding of free enzyme (E) to substrate (S) to create an ES complex (Michaelis and Menten, 1913). If one of these steps in the overall reaction pathway that precedes the transformation step is rate-limiting or partially rate-limiting, the AKIE may be suppressed relative to the intrinsic KIE (Northrop, 1981; O’Leary, 1989), known as a “masking effect”. Masking effects have been shown to occur due to a variety of phenomenon, including transport through cell membranes (Ehrl et al., 2018; Nijenhuis et al., 2005; Thullner et al., 2013), trace element abundance vs. limitation (Mancini et al., 2006), and enzyme-substrate binding (Sherwood Lollar et al., 2010; Świderek and Paneth, 2013).

CSIA measures stable isotope ratios of an element ($R = {}^H E / {}^L E$), typically expressed in δ notation in per mille (‰; Eq. 1):

$$\delta^H E = (R_{\text{sample}} / R_{\text{standard}}) - 1 \quad \text{Eq. 1}$$

where R_{standard} is the isotopic ratio of an international reference standard for the element of interest (e.g., Vienna Pee Dee Belemnite (V-PDB) for carbon, Standard Mean Ocean Chloride (SMOC) for chlorine (Hunkeler et al., 2008 and references therein). Dual-isotope analysis, where stable isotopes of two different elements within the same molecule are analyzed, is a powerful tool that can overcome masking effects (recently reviewed by Ojeda et al. (2020) and Kuntze et al. (2019)). Dual-isotope plots show the absolute fractionation of one element (e.g., carbon, $\Delta\delta^{13}C$), against another (e.g., chlorine, $\Delta\delta^{37}Cl$), which generally produces a linear relationship with a slope, Λ . If a masking effect is present that does not isotopically fractionate either element, both elements will be suppressed to a similar extent, and Λ will therefore be unaffected by masking (recently reviewed in Ojeda et al. (2020)). As such, Λ values give more

robust insight into the kinetics and reaction mechanisms for enzymatic transformation than fractionation effects measured for only one element. Mechanistic investigations using CSIA also benefit from comparing biological fractionation effects to abiotic reference experiments, for example in studies where abiotic corrinoids are compared to RDases containing catalytically active corrinoids (cobamides) (Heckel et al., 2019; Lihl et al., 2019; Renpenning et al., 2014; Rodríguez-Fernández et al., 2018). The protein environment (e.g. amino acid residues in the vicinity of the active site) and structure are also important parameters, as studies of other classes of enzymes containing earth abundant metals (EAMs) at their core have their reactivity modulated by the surrounding protein environment (as reviewed by Bullock et al. (2020)).

Previous work (Chan et al., 2012; Heckel et al., 2019; Lee et al., 2015; Soder-Walz et al., 2022) using CSIA to investigate biotransformation of CF is shown in Table 1. Significant differences in both carbon and chlorine isotope effects were observed for different enrichment cultures. Even for cultures that all contain the same organism, *Dehalobacter restrictus* (*Dhb*), different strains and their associated enzymes, such as strain CF with RDase CfrA (Tang and Edwards, 2013), strain UNSWDHB with RDase TmrA (Wong et al., 2016); and KB-1® Plus with CF-rdhA, show significant differences (Table 1). Like observations for substrate specificity within OG 97 (discussed above), differences in isotope fractionation during biotransformation can even be observed for two enzymes (e.g., CfrA and TmrA) that have high similarity (>95%) at the amino acid level (Lee et al., 2015; Table 1). Carbon isotope effects produced by biotransformation of CF can differ significantly (this study; Heckel et al., 2019) and chlorine isotope effects differ in magnitude as well as direction (this study; Heckel et al., 2019; Table 1). The differences in AKIE_C and AKIE_{Cl} produce differences in dual-isotope plots (Table 1), e.g., $\Lambda_{C/Cl} = 3.39 \pm 0.15$ for CfrA and $\Lambda_{C/Cl} = -1.2 \pm 0.2$ for TmrA. Differences for *D. restrictus* strain

UNSWDHB have been observed in mixed culture (CFH2) (Lee et al., 2015), in isolated *D. restrictus* strain UNSWDHB (Heckel et al., 2019), and in cell-free extracts (Heckel et al., 2019). It remains unknown whether CF biotransformation proceeds via a direct interaction between the cobalt atom of the cobamide (e.g. bimolecular nucleophilic substitution (S_N2)), or by electron transfer (IS-SET or OS-SET) (Heckel et al., 2019), and the explanation for the significant differences in fractionation is still lacking to date.

Nonetheless by compiling all the available data above (and in Table 1) this paper will demonstrate some consistent patterns that inform understanding of the different enzymes and the observed variations in fractionation. Importantly where carbon isotope results were run for the same culture and strain, even over almost a decade, the same results for ϵ_c were found within uncertainty (Table 1 ACT-3 results for 3 separate studies). Secondly, all data to date confirm that different cultures, different strains, and enzymes, can exhibit very different fractionation, with much smaller ϵ_c values observed for other cultures and strains (Table 1 – shaded orange) compared to those observed for ACT-3 and for abiotic transformation in Vitamin B₁₂ (Table 1 – shaded green). Third and most importantly, when ϵ_c values are large, ϵ_{Cl} values are also large (shaded green data in Table 1), while conversely, experiments showing smaller ϵ_c values also show smaller ϵ_{Cl} values (shaded orange data in Table 1) (and correspondingly smaller Δ values where multi-element isotope data are run). This study provides insights to understand these large-scale variations in the current study and the literature to date, and to suggest further lines of investigation that should be undertaken to advance this area of inquiry further.

KB-1[®] Plus CF is an enriched microbial culture that is maintained and marketed by SiREM as part of its KB-1[®] Plus line of bioaugmentation cultures. Like the enrichment culture CFH2 (Lee et al., 2015), KB-1[®] Plus CF is an enrichment culture that dechlorinates CF to DCM,

as well as further fully dechlorinating and oxidizing DCM to CO₂ (Wang et al., 2022). KB-1[®] Plus CF contains a *Dehalobacter* strain with a gene likely responsible for CF transformation (KB-1[®] Plus CF -rdhA). KB-1[®] Plus CF is a “self-sustaining” culture, where DCM transformation produces H₂ that is used as an electron donor for CF transformation (Wang et al., 2022). No previous work has reported carbon or chlorine isotope effects for transformation of organohalides by KB-1[®] Plus CF. Here, we use carbon and chlorine CSIA to investigate the isotope effects during biotransformation of CF by the enriched microbial culture KB-1[®] Plus CF and compare to those observed for other CF dechlorinating organisms containing chlorinated alkane degrading RDases in OG 97. Furthermore, we compare the amino acid sequence identity of all the known RDases in OG 97 to investigate the relationship between isotope fractionation and active site amino acid composition of chlorinated alkane degrading RDases (Molenda et al., 2020). The objective is to investigate relationships between genetic sequences, enzyme activity, and observed isotope fractionation. In addition to providing a better understanding of the links between protein structure and enzyme activity, this investigation will, in the short-term, provide better characterization of stable isotope fractionation associated with biotransformation of these priority contaminants and a more robust basis for using CSIA to determine biotransformation efficiency and rates of clean-up from contaminated field sites.

Materials and Methods

Amino Acid Alignments and Protein Models.

The KB-1[®] Plus CF *rdhA* sequence was identified from metagenome data (publication TBD, see full sequence in S.I. Section 3) using BLAST (Altschul et al., 1990) and found highly similar sequences to the published *cfrA* sequence (Accession: [AFV05253](#); Tang et al., 2012). The

query *cfrA* sequence was aligned to the top BLAST hit (Bit score: 2399.92, HSP score: 1299, E-value: 0, Mismatches: 2) using MUSCLE to determine amino acid differences (Edgar, 2004). Amino acid sequence alignments for RDases in OG 97 were prepared in Geneious 8.1.9 using the MUSCLE plugin (Edgar, 2004) to align the published sequences of ThmA (Accession No.: ANI21407), CtrA (AGO27983), TmrA (WP_034377773), CfrA (AFV05253), and DcrA (WP_015043247); (Deshpande et al., 2013; Tang et al., 2012; Zhao et al., 2017, 2015). A fifth sequence corresponding to the KB-1[®] Plus CF RdhA is provided in the S.I. (Section 3), along with a full sequence comparison to the ACT-3/CF RDase. Alignments of the specific amino acids within the predicted active site/binding pocket (predicted using protein models, discussed below) are shown in Figure 3.

Protein structure models of each sequence were created using Robetta, a protein structure prediction service that creates a 3D protein structure when provided an amino acid sequence (Kim et al., 2004). As such they are not unique to a specific substrate. Quality metrics are then used to evaluate whether the modelled proteins are feasible in nature based on steric interactions between residues and how the amino acids are bent. Modelling is accomplished using RoseTTAFold, a deep learning-based method that is top-ranked as evaluated through CAMEO (Baek et al., 2021). The quality of each structure prediction was assessed with MolProbity (Williams et al., 2018) and visualized in PyMOL (Schrödinger LLC, 2021) (details in SI and Table S3). Using Robetta, the location of the cofactor within the protein can be approximated by comparing to previously published structures. It is well known that protein structures are much more conserved than the amino acid sequence to retain protein functionality. Unfortunately no experimentally determined structures exist for this group of reductive dehalogenases (RDases in OG 97). However, comparing the Robetta derived predictions for the RDases to experimentally

determined structures for other enzymes do show some similarities. Specifically, comparisons can be made to the homologous *Nitratireductor pacificus* pht-3B catabolic reductive dehalogenase (NpRdhA, 20.9% amino acid identity to CfrA) crystal structure (Payne et al., 2015). Despite there being a sequence similarity of only 20-30% between the experimentally determined structures and the modelled structures in OG 97, it is apparent that the RDase family shares similarities (a conserved fold) within their active site. This conserved fold is also seen between the experimental structures of NpRdhA and those of PceA which only share 21% sequence similarity (Bommer et al., 2014). This similarity in structures permits approximation of the location of the cofactor in the modelled proteins in OG 97 by superimposing the cofactor location using the known NpRdhA structure and hence visualization of the predicted active site. In this work, this allowed approximation of the amino acids that are in the active site of the RDases in OG 97. The models were used to predict which amino acid residues are in the predicted active sites, which are then compared (i.e. Figure 3). The models generated using the deep learning algorithm (RoseTTAFold) can be assessed by a series of quality scores, established by a structure-validation web service (MolProbity) explained in more detail in the SI and Table S3.

Cultures and Growth Conditions.

Biotransformation experiments were performed for CF biotransformation by enrichment culture ACT-3/CF and KB-1® Plus CF. The parent culture (ACT-3) is derived from contaminated aquifer material from a 1,1,1-TCA-contaminated site in the northeastern United States (Grostern and Edwards, 2006) and has been maintained for more than 10 years in minimal mineral salt medium amended with 1,1,1-TCA as an electron acceptor, with an electron donor mix of either MEAL (methanol, ethanol, acetate, and lactate) or EL (ethanol, lactate). This

culture contains *Dehalobacter restrictus* strain CF that dechlorinates CF to DCM (strain CF) linked to growth using CfrA (Grostern and Edwards, 2006). A sub-culture, ACT-3/CF has been maintained on chloroform (CF) as the electron acceptor with ethanol and lactate as electron donors for 4 years in minimal mineral salt medium (Edwards and Grbic-Galic, 1994). For experiments with the KB-1® Plus CF, a culture aliquot was provided by SiREM Laboratories (Guelph ON). KB-1® Plus CF is an enriched microbial culture containing *Dehalobacter* that was derived from a site in California with both trichloroethylene (TCE) and CF contamination (Wang et al., 2022). The enriched parent culture has been maintained since 2010 at SiREM in defined mineral medium (Edwards and Grbić-Galić, 1992) amended periodically with CF as the electron acceptor. The aliquot of KB-1® Plus CF was maintained at the University of Toronto with an initial addition of CF with electron donor (solution of HPLC grade ethanol and lactate) and subsequent refeeding with CF only.

Microcosm Setup.

For biotransformation experiments, triplicate glass serum vials (Bellco Glass Inc.™) with a total volume of 550 mL each were prepared in an anaerobic glovebox (Labconoco™) with CO₂/H₂/N₂ atmosphere (10%/10%/80%). The triplicate bottles were then filled with 500 mL of enriched anaerobic microbial culture, either ACT-3/CF or KB-1® Plus CF, in a defined mineral medium (Edwards and Grbić-Galić, 1992). A sterile control containing 500 mL of autoclaved culture was prepared for each experiment and measured to ensure that the isotopic compositions were not affected by experimental design or sampling procedure. Each bottle was amended with a solution of HPLC grade ethanol and lactate (0.3 mL of a solution with 200 mM ethanol and 200 mM lactate) and 41 µL of CF to produce 1 mM aqueous concentration. These amendments provided a 5-fold excess of donor relative to reductive dechlorination. The CF stock was

characterized using offline preparation and dual inlet measurement ($\delta^{13}\text{C} = -49.8 \pm 0.1\text{‰}$ based on Vienna Pee-Dee-Belemnite, V-PDB). Bottles were then capped with blue butyl stoppers (Bellco Glass Inc.TM) that were pre-treated by boiling in 0.1M solution of NaOH for 1 hour and rinsed with deionized water (after the method of Ward et al., 2004). Triplicate bottles were stored on their side in the anaerobic chamber for five hours to ensure complete equilibration between the aqueous and gaseous phases before analysis, as determined in laboratory protocol tests. At each time point of the experiment, 4-7 mL aqueous samples were withdrawn for isotope analysis from each replicate and control bottle using a glass syringe (Hamilton®), and the volume was replaced with fresh media. Samples were added to 5-mL or 8-mL glass vials containing 1 mL of 1 M sulfuric acid to create a total volume of 5 mL or 8-mL and capped with a PTFE-lined cap. Samples were stored and shipped at 4°C and kept upside down prior to analysis. Protein was extracted from KB-1® Plus CF to confirm the expression of KB-1® Plus CF RdhA using an adapted protocol (Murdoch et al., 2021). Details on protein extraction and analysis are provided in the S.I. Section 1.

Analytical Methods.

Detailed analytical methods are presented in the S.I. Section 1. Briefly, CF and DCM concentrations were quantified using a Varian 3400 gas chromatograph (GC) equipped with a flame ionization detector (FID). Three-point calibration curves for CF and DCM were prepared and checked daily with standards. Samples were run in duplicate and mean values are reported based on reproducibility always better than $\pm 5\%$. Carbon isotope measurements were performed on a Finnigan MAT 253 IRMS. Isotopically characterized laboratory isotopic standards CF ($\delta^{13}\text{C} = -47.10 \pm 0.14\text{‰}$) and DCM ($\delta^{13}\text{C} = -52.85 \pm 0.27\text{‰}$) were tested daily to confirm accuracy. The total uncertainty of $\delta^{13}\text{C}$ measurements is $\pm 0.5\text{‰}$ incorporating both accuracy and

reproducibility (Hunkeler et al., 2008; Sherwood Lollar et al., 2007). Chlorine isotope measurements were performed on a Neptune MC-ICPMS (Thermo Fisher Scientific, Germany) interfaced with a Thermo Scientific Trace 1310 GC after the method of Renpenning et al. (2018). Three offline characterized in-house standards (measured using DI-IRMS) were used to normalize sample measurements on the SMOC scale and ensure accuracy; methyl chloride (MC, $\delta^{37}\text{Cl} = +6.02\text{‰}$), and two different trichloroethenes (TCE2, $\delta^{37}\text{Cl} = -1.19\text{‰}$, and TCE6 $\delta^{37}\text{Cl} = +2.17\text{‰}$) (Renpenning et al., 2015a). The maximum reproducibility (1σ) observed for sample and control measurements was less than $\pm 0.3\text{‰}$.

One technical issue that is noted here is the larger degree of inter-laboratory variability in chlorine isotope results than for carbon (ϵ_{C} for CF biotransformation by CfrA in ACT-3 between this study and Heckel et al. 2019, Table 1). Specifically, while the three sets of experiments run for carbon isotopes for ACT-3 at three different laboratories (Toronto, Leipzig, Munich) all returned the same value of ϵ_{C} within uncertainty, the chlorine isotope results for this study run at UFZ Leipzig (MC-ICP-MS) are outside uncertainty compared to those run by colleagues at Munich (GC-IRMS) from Heckel et al. (2019) (see S.I. for more details on the cross-calibration and standards used between these two laboratories). Importantly, these analytical differences detailed in the S.I. do not affect the major findings of the current study. First, the main interpretational focus of this paper is a comparison of the two new sets of data (indicated in bold in Table 1) with consistent carbon isotope effects and run by the same chlorine isotope lab (UFZ Leipzig), thereby ensuring they are directly inter-comparable. Secondly, the main finding, that both carbon and chlorine isotope fractionation for CF biotransformation by ACT-3 and for abiotic baseline reference experiments (green shaded data Table 1), are large compared to all other published results (orange shaded data Table 1) remains robust regardless of the differences

in the absolute values of ϵ_{Cl} from this study versus Heckel et al. (2019) for ACT-3 (see S.I. for further details).

Calculations

The isotopic ratio of a contaminant undergoing transformation can be related to the fraction of original parent remaining using the Rayleigh model (Eq. 2):

$$\ln(R/R_0) = \epsilon_E * \ln(f) \quad \text{Eq. 2}$$

where, in contaminant hydrogeology R_0 is the initial isotopic composition of the parent contaminant, f is the fraction of original contaminant remaining, and ϵ_E is the isotopic fractionation (in ‰), which describes the magnitude of isotopic fractionation for a given reaction and is equal to $(1/(KIE) - 1)$ (see Mariotti et al. 1981). The KIE reflects the primary isotope effect of the reacting bond and ϵ_E are measured using bulk molecules, thus ϵ_E are typically converted to AKIE values (see S.I. Eq. 4) to account for the effects of non-reactive positions, intramolecular isotope distributions and intramolecular competition (Elsner et al., 2005). All uncertainty is reported to two significant figures and the measured or calculated value is reported to the same digit as the uncertainty, as per best practice guidance recommendations (Joint Committee for Guides in Metrology, 2008; NIST, 2019). More detail on calculations is provided in the S.I. Section 1.

Results and Discussions

Highly Similar Proteins Show Substantial Differences in Carbon and Chlorine Isotope Fractionation.

Expression of the KB-1® Plus CF RdhA was confirmed through proteomics (log(e) = -252). Rayleigh plots of carbon and chlorine isotopic data, and dual-isotope results are given in Figure 1. Table 1 shows a comparison of available AKIE values for chlorinated alkane transforming RDases in OG 97. Both carbon ($\epsilon_C = -1.52 \pm 0.34\%$) and chlorine ($\epsilon_{Cl} = -1.84 \pm 0.19\%$) ϵ for biotransformation of CF by KB-1® Plus CF are significantly smaller compared to those reported for biotransformation of CF by ACT-3/CF (see results from Table 1 both from this study and Heckel et al. 2019) and compared to those of an abiotic reference system (Table 1; Heckel et al. 2019). This smaller fractionation in both carbon and chlorine isotopes compared to both abiotic transformation experiments and experiments with ACT-3 could theoretically be attributed to a masking effect in the KB-1® Plus CF experiments. Dual-isotope plots also show different $\Lambda_{C/Cl}$ ($\Lambda_{C/Cl} = 3.39 \pm 0.50$ for ACT-3 containing CfrA and $\Lambda_{C/Cl} = 1.13 \pm 0.35$ for KB-1® Plus CF containing KB-1® Plus CF RdhA). The KB-1® Plus CF results are even more suppressed compared to the $\Lambda_{C/Cl}$ value from Heckel et al. (2019), The significantly smaller ϵ_C , ϵ_{Cl} , and $\Lambda_{C/Cl}$ observed during biotransformation of CF by KB-1® Plus CF compared to ACT-3 thus suggests either the presence of an additional rate-limiting (masking) step that fractionates carbon and/or chlorine isotopes, or possibly a different reaction mechanism. Similar strains of *Dehalobacter* are responsible for CF dechlorination in the ACT-3 and KB-1® Plus CF cultures, and thus likely have identical cell wall structures, making transport across the outer membrane unlikely as a rate-limiting step contributing to masking.

Consistent with this reasoning, transport across the outer membrane was ruled out as a cause for differences in isotope effects produced for CF transformation by two *Dehalobacter* strains in a prior study (Heckel et al., 2019). Furthermore, masking effects due to transport into the periplasm in *Dehalobacter restrictus* were not observed during trichloroethene (TCE) transformation (Renpenning et al., 2015b). Renpenning et al., (2015b) attributed the observed masking in that study to differing degrees of hydrophobicity of the substrate (with more hydrophobic substrates demonstrated a higher degree masking). Extrapolating this principle suggests CF would show a lower degree of masking than TCE since CF is less hydrophobic (based on organic water partitioning coefficients, K_{OW} , 93) compared to TCE ($K_{OW} = 407$). The differences between the isotope effects observed for biotransformation of CF by ACT-3 and KB-1® Plus CF are likely either due to mechanistic differences or due to other additional rate-limiting steps, such as binding of enzyme to substrate, or electron flow from the donor, causing differing extents of isotope fractionation suppression in carbon and chlorine to produce different dual-isotope slopes.

Insert Figure 1.

The sequences of CfrA and KB-1® Plus CF RdhA share over 95% similarity at the amino acid level (Figure 2). Despite this high similarity, carbon and chlorine isotope effects observed during biotransformation of CF by these two cultures containing CfrA and KB-1® Plus CF RdhA are significantly different, as discussed above (Figure 1, Table 1). Both cultures biotransform CF via hydrogenolysis to dichloromethane (DCM), however KB-1® Plus CF shows significantly smaller carbon and chlorine isotope effects relative to ACT-3 (Figure 1, Table S1). Similarly, carbon and chlorine isotope effects observed for CfrA and TmrA are significantly different (Table 1) despite sharing > 95% amino acid sequence identity (Lee et al., 2015). The substrate

preferences of these enzymes are consistent when heterologously expressed (Picott et al., 2022), indicating that differences in substrate preferences are at the enzyme level, and not due to differences in the host organism's respiratory pathway. For transformation of chlorinated ethenes similar observations have been made (Büsing et al., 2020; Lihl et al., 2019) suggesting differences in isotope fractionation between different RDases in OG 97 may be controlled by a small subset of amino acid residues as well.

Insert Figure 2.

Amino Acid Similarity Between Reductive Dehalogenases.

The CfrA and the KB-1® Plus CF RdhA sequences differ in only 19/456 amino acids (95.8% similarity, Figure 2). A comparison of the entire protein amino acid compositions for the enzymes is presented in the S.I. (Figure S1). While none of the enzymes within OG 97 have been structurally determined through crystallization, protein structures can be predicted through protein modelling servers like Robetta, which harnesses a deep learning-based method, RoseTTAFold, to determine structure from sequence (Baek et al., 2021). Previous structural studies of homologous RDases PceA and NpRdhA demonstrated a conserved fold within the RDase active structure that forms the buried active site (Bommer et al., 2014; Kunze et al., 2017; Payne et al., 2015). By superimposing the CfrA and KB-1® Plus CF RdhA structure models to the NpRdhA crystal structure, the amino acid residues in the active sites of CfrA and the KB-1® Plus CF RdhA were predicted and compared to those in other OG 97 RDases (Figure 3 and Figure S1 for full alignment). Four residues differ between the active sites of CfrA and KB-1® Plus CF RdhA (indicated with '*' in Figure 3). Despite the differences in substrate specificity and isotope fractionation observed for all reductive dehalogenases in OG 97, the active site residues are highly conserved except for five residues, including the four variable locations

between CfrA and KB-1® Plus CF RdhA (highlighted in Figure 3). While the models of the other enzymes in OG 97 are not shown here, quality scores of these models (used to confirm that residues in Figure 3 are within predicted active sites) are given in Table S3.

Amino acid mutations, even at a single location, have been shown to result in significant effects on substrate specificity and enzyme activity of the active sites for a variety of enzymes (reviewed by Currin et al., 2015). For example, a single mutation in the LovD enzyme increased the kinetics of the transformation step of acyl transfer (k_{cat}) tenfold (Jiménez-Osés et al., 2014). Further, three active site mutations in LovD were suggested to significantly stabilize the enzyme in an optimal catalytic state (Jiménez-Osés et al., 2014). While such amino acid mutations can have pronounced effects on catalysis, these effects are not necessarily dependent on distance from the active site (Morley & Kazlauskas, 2005). In contrast to effects on catalysis, mutations proximal to the active site have a strong impact on substrate specificity, likely due to impacts on substrate binding (Paramesvaran et al., 2009).

Insert Figure 3.

Correlating Active Site Amino Acid Alignments with Mechanisms and Isotope Effects.

This study investigated differences in carbon and chlorine isotope effects for CF biotransformation (Table 1) by chloroalkane reductive dehalogenases in OG 97 and the relationship to the five variable amino acids at their active site (indicated by coloured residues in Figure 3). Locations of the variable residues between CfrA (ACT-3/CF) and KB-1® Plus CF RdhA (indicated by “*” in Figure 3) within the proteins can be determined through sequence alignment and visualized using three-dimensional protein models (Baek et al., 2021) to derive three-dimensional structures from the primary amino acid sequences (Figure 4). The amino acids

in the four variable locations between CfrA and KB-1® Plus CF RdhA differ in properties such as the potential for hydrogen bonding (location Y80 vs F80, M391 vs. W391), polarity (C260 vs. Y260), and aromaticity (location C260 vs. Y260, L388 vs. F388, M391 vs. W39; Table S2). Bulkier residues (e.g. aromatic residues) are observed in the active site of KB-1® Plus CF RdhA (shown in orange in Figure 4B, D) compared to CfrA (ACT-3/CF; shown in pink in Figure 4A, C). Active sites crowded by amino acid residues have been suggested as evidence for long range electron transfer in structural studies (Bommer et al., 2014; Payne et al., 2015). As discussed in more detail below, carbon and chlorine isotope fractionation for biotransformation of CF by KB-1® Plus CF RdhA are inconsistent with abiotic long-range electron transfer reference experiments (Heckel et al., 2017). Although interpreting the effects of amino acid differences on reaction mechanisms cannot be directly made based on the data available, the greater number of atoms in the side chains in the aromatic residues in KB-1® Plus CF RdhA compared to CfrA could potentially create a more crowded enzymatic pocket. In such a case the substrate may be positioned in a different way, leading to differences in the bonding in the transition state and hence, different isotope effects. In contrast, active sites containing fewer aromatic functional groups result in more flexibility in interaction of the cobalt atom (Co, within corrinoid) and halogenated substrate (R-X) by facilitating direct Co-R interaction in an S_N2 mechanism. Such an enhanced interaction would be consistent with the large carbon and chlorine isotope effects observed for CfrA. A previous study (Heckel et al., 2019) demonstrated large carbon and chlorine isotope effects during biotransformation of CF by ACT-3 like those observed during transformation by abiotic vitamin B₁₂ and proposed an S_N2 mechanism for this process. While both CfrA and KB-1® Plus CF RdhA likely contain vitamin B₁₂ as a cofactor (both cultures were grown with vitamin B₁₂ in the medium), it is possible that the transformation mechanisms of

abiotic vitamin B₁₂ differ from vitamin B₁₂-containing RDases depending on the protein environment.

Previous literature includes crystallization structures of PceA with its native cobamide in chlorinated ethene transformation (Bommer et al., 2014). Bommer et al. (2014) proposed that formation of a carbon-cobalt bond after a nucleophilic attack was unlikely based on spatial restrictions within the PceA active site for TCE transformation, however the authors were not able to specify the reaction mechanism. Isotope studies of PceA under the same conditions (Renpenning et al., 2014) produced highly suppressed carbon ($\epsilon_C = -1.4 \pm 0.1\%$) and chlorine ($\epsilon_{Cl} = -0.6 \pm 0.2\%$) relative to the same abiotic corrinoid ($\epsilon_C = -25.3 \pm 0.8\%$, $\epsilon_{Cl} = -3.6\% \pm 0.4$) for PCE transformation. In contrast, similar ranges were observed for enzymatic TCE transformation ($\epsilon_C = -20.0 \pm 0.5\%$, $\epsilon_{Cl} = -3.7\% \pm 0.2$) compared to abiotic corrinoids ($\epsilon_C = -15\%$ to -18.5% , $\epsilon_{Cl} = -3.2\%$ to -4.2%). Although long-range electron transfer has been proposed as a mechanism for PceA-catalyzed reductive dechlorination of brominated phenols, the isotope effects observed for enzymatic reductive dechlorination of PCE and TCE (given above, Renpenning et al., 2014) are inconsistent with abiotic reference experiments for outer sphere electron transfer of PCE ($\epsilon_C = -7.6\%$ to -15.4% , $\epsilon_{Cl} = 0.05\%$ to -1.5%) and TCE ($\epsilon_C = -11.9\%$ to -27% , $\epsilon_{Cl} = 0.04\%$ to -2.5% ; Heckel et al., 2017). An analysis of the abiotic corrinoid mechanism for chlorinated ethene transformation (Heckel et al., 2018) supported a first step involving direct Co-R interaction to form an adduct. Taken together, spatial restrictions within the PceA active site may be related to suppressed isotope effects observed for PCE enzymatic transformation, either due to masking effects or differences in reaction mechanisms between the abiotic corrinoid alone (abiotic) and the active enzyme (biotic) influenced by the protein environment: nucleophilic addition with subsequent elimination for the abiotic corrinoid

(producing large C and Cl isotope effects); while the PceA enzyme uses a yet unidentified mechanism (producing suppressed C and Cl isotope effects).

Differences in mechanisms between CfrA (ACT-3/CF) and KB-1® Plus CF RdhA may also arise due to the residues in their active sites, influencing the observed differences in C and Cl isotope effects. As discussed earlier, CF biotransformation by ACT-3/CF likely proceeds via an S_N2 mechanism, while KB-1® Plus CF biotransformation of CF may proceed via a distinct, unidentified mechanism producing suppressed C and Cl isotope effects (Table S1, Figure 3). The carbon and chlorine isotope effects for CF biotransformation by KB-1® Plus CF RdhA are inconsistent with abiotic reference experiments for outer sphere electron transfer ($\epsilon_C = -17.7 \pm 0.8 \text{ ‰}$, $\epsilon_{Cl} = 2.6 \pm 0.2 \text{ ‰}$) from Heckel et al. (2017). The protein models (Figure 4) predict that the differences in the amino acids between CfrA and KB-1® Plus CF RdhA are within the RDase active sites. Since these two enzymes also show differences in the carbon and chlorine isotope effects observed for biotransformation of chlorinated alkanes in OG 97, these two sets of observation (active site differences, and differences in fractionation) suggests these phenomena could be related. It is possible that the differences the amino acids in the RDase active site result in different reaction mechanisms and/or an additional rate-limiting step that involves fractionation, either of which could result in the varying C and Cl isotope effects between RDases in OG 97 (i.e. Figure 5). Certainly, the findings of this study suggest the relationship between the amino acid alignments, protein structures, and fractionation should be the focus of additional investigation in future studies. While masking of the isotope effect due to enzyme substrate binding or electron shuttling within the enzyme because of different amino acids between CfrA (ACT-3/CF) and KB-1® Plus CF RdhA cannot be ruled out, as noted previously such a change in the binding would also have to be isotopically fractionating to explain the

differences in C and Cl isotope effects for biotransformation of CF by ACT-3/CF and KB-1® Plus CF.

Insert Figure 4.

Patterns of C and Cl Isotope Effects Correspond to Similarities in Amino Acid Residues.

As discussed in the introduction, a compilation of all isotope fractionation studies to date for CF biotransformation (Table 1) shows significant variability but some important consistent patterns. First and foremost, different cultures containing different strains of *Dehalobacter restrictus* and different enzymes show different isotope fractionation results for both carbon and chlorine. Second the fractionation correlates such that results fall into two groups – those with high coupled carbon and chlorine isotope fractionation (shown in green in Table 1); and those where both carbon and chlorine isotope fractionation are low (shown in orange in Table 1). Despite some variability from laboratory to laboratory that should be explored through inter-laboratory cross-calibration, especially for chlorine isotope results, these patterns of large and small fractionation, and hence large and small AKIE values, are a consistent observation based on results from all the groups and publications appearing to date (Figure 5).

Further these patterns extend to stable isotope fractionation studies done for other chlorinated compounds, specifically 1,1,1-TCA and 1,1-DCA (Figure 5). Comparing published carbon and chlorine isotope effects using AKIE, isotope results observed during biotransformation by RDases in OG 97 can be broadly distinguished into two groups, those with moderate to high C and Cl isotope effects ($AKIE_C > 1.01$ and $AKIE_{Cl} > 1.008$), including CfrA and DcrA, and those with low C and Cl isotope effects ($AKIE_C < 1.01$ and $AKIE_{Cl} < 1.008$), including TmrA and KB-1® Plus CF RdhA. TmrA, KB-1® Plus CF RdhA, and strain 8M (with

a yet uncharacterized RDase) produce smaller carbon and chlorine isotope effects for CF transformation. These smaller isotope effects may correspond to similarities in the amino acids at residues 80 (F), 388 (F) and 39 (W) (Figure 3, Figure 5), residues common to TmrA and KB-1® Plus CF RdhA that are different from CfrA, suggesting these amino acid residues may influence the observed isotope effects for OG 97 RDases, either by influencing reaction mechanisms or isotopically fractionating masking effects (such as enzyme-substrate binding or rate-limiting electron shuttling in the enzyme).

Insert Figure 5.

Based on the observations in this study, the carbon and chlorine isotope effects produced by CtrA may be like those of CfrA due to the similarities in their amino acids at residues 260 (C) and 388 (L) (Figure 3). If CtrA carbon and chlorine isotope effects are different from those observed for CF transformation by CfrA, this would indicate that the differences at residues 80 and 391 influence the reaction mechanism or the presence of an additional, fractionating rate-limiting step for biotransformation of chlorinated methanes. Similarly, strain 8M shows suppressed carbon and chlorine isotope effects (Soder-Walz et al., 2022), close to what is observed for TmrA and KB-1® Plus CF RdhA (Table 1, Figure 5). This RDase has not been identified, characterized genetically or biochemically, however if further characterization occurs showing the same residues at locations 80 (F), 388 (F) and 391 (W), this would be a helpful test of the influence of these residues on carbon and chlorine isotope effects. Testing these hypotheses through transformation experiments with CtrA and characterization of the RDase in strain 8M is outside of the scope of the present work but represent important future steps in further refining this hypothesis. Further characterization of carbon and chlorine isotope fractionation of all known substrate ranges within OG 97, along with testing more substrates to

confirm if these enzymes are active, would advance the understanding of the mechanisms of RDases within this OG. Despite this, these initial observations suggest that differences in substrate ranges and observed isotope fractionation for the RDases within OG 97 may be related to key amino acid differences within the active sites of these enzymes.

Relevance for Interpreting CSIA Data in Environmental Remediation.

A better understanding of what controls substrate specificity, activity, and reaction mechanisms of reductive dehalogenases can be used to optimize remediation strategies, e.g., to help practitioners evaluate whether native microbes present at a contaminated site can break down the contaminants present or to select appropriate microbes for bioaugmentation. CSIA is a powerful tool that can be used to gain insights into RDase behavior, and this work demonstrates an innovative integration of CSIA data with RDase classification based on amino acid similarity (into OGs). The substantial differences observed in carbon and chlorine isotope fractionation, despite high similarity at the amino acid level for two cultures with active RDases, provide insight into the role of specific residues in the RDase structure controlling either transformation mechanisms or masking effects (e.g. enzyme-substrate binding or electron shuttling). These findings highlight specific locations in the active sites of RDases that should be further investigated, e.g., through structural analysis and/or site-specific mutagenesis, to gain further insights into RDase structure and function. ACT-3 and KB-1® Plus CF are both commercially available cultures, and the estimates of $\Lambda_{C/Cl}$ and $\epsilon_{E, bulk}$ reported here can be applied at sites where these cultures are augmented as a remediation strategy, or where their RDases (CfrA, KB-1® Plus CF RdhA) are detected. This is particularly important for KB-1® Plus CF RdhA, as the terminal degradation product (CO₂) is a non-unique product, and thus daughter product characterization cannot reliably be used to confirm biotransformation in the field. An important

implication of this work is that high amino acid similarity alone between two RDases should not be used as a basis to approximate $\epsilon_{E, \text{bulk}}$ and $\Lambda_{C/Cl}$ values. Determining the role of residues in RDase structure that affect the observed isotope effect during RDase dechlorination activity may provide more detailed context on reaction mechanisms to aid in predicting isotope effects using computations of reaction coordinates and transition state structures. Such information can give practitioners the tools to better estimate appropriate $\epsilon_{E, \text{bulk}}$ values to estimate rates and extents of transformation. $\Lambda_{C/Cl}$ was not consistent for biotransformation of CF by ACT-3 (3.39 ± 0.16) and KB-1® Plus CF (1.13 ± 0.35), indicating that reductive dechlorination of CF either reflects a large range of $\Lambda_{C/Cl}$ values, or that there may be different mechanisms of CF hydrogenolysis which produce different $\Lambda_{C/Cl}$, similar to what has been proposed for hydrogenolysis of chlorinated ethenes (Heckel et al., 2018; Lihl et al., 2019). An improved understanding of RDase function and the cause of these differing $\Lambda_{C/Cl}$ values would significantly improve the reliable identification of reaction pathways using dual-isotope analysis and hence improve the design, implementation, and optimization of biotransformation as a remediation strategy for contaminated groundwater.

Acknowledgements

Funding for this study was provided by Canada Research Chair and NSERC Discovery Grants to BSL with additional funds from Agriscience Canada. We are thankful for the use of the analytical facilities of the Centre for Chemical Microscopy (ProVIS) at the Helmholtz Centre for Environmental Research – UFZ supported by European Regional Development Funds (EFRE – Europe funds Saxony) and the Helmholtz Association. We are grateful to Robert Flick for proteomics analysis and processing. Additional supporting funding from CIFAR Earth4D for which BSL is Co-Director and Fellow is acknowledged.

Associated content

The Supporting Information is available free of charge on the Oxford University Press website.

References

- Adrian, L., Löffler, F.E., 2016. Organohalide Respiring Bacteria - An Introduction, in: Adrian, L., Löffler, F.E. (Eds.), Organohalide-Respiring Bacteria. Springer-Verlag, Berlin, pp. 3–7.
- Altschul, S.F., Gish, W., Miller, W., Myers, E.W., Lipman, D.J., 1990. Basic local alignment search tool. *Journal of Molecular Biology* 215, 403–410. [https://doi.org/10.1016/S0022-2836\(05\)80360-2](https://doi.org/10.1016/S0022-2836(05)80360-2)
- Baek, M., Dimaio, F., Anishchenko, I., Dauparas, J., Ovchinnikov, S., Lee, G.R., Wang, J., Cong, Q., Kinch, L.N., Schaeffer, R.D., Millán, C., Park, H., Adams, C., Glassman, C.R., Degiovanni, A., Pereira, J.H., Rodrigues, A. v, van Dijk, A.A., Ebrecht, A.C., Opperman, D.J., Sagmeister, T., Buhlheller, C., Pavkov-Keller, T., Rathinaswamy, M.K., Dalwadi, U., Yip, C.K., Burke, J.E., Garcia, K.C., Adams, P.D., Read, R.J., Baker, D., 2021. Accurate prediction of protein structures and interactions using a three-track neural network, *Science*.
- Bigeleisen, J., 1949. The relative reaction velocities of isotopic molecules. *The Journal of Chemical Physics* 17, 675–678. <https://doi.org/10.1063/1.1747368>
- Bommer, M., Kunze, C., Fessler, J., Schubert, T., Diekert, G., Dobbek, H., 2014. Structural basis for organohalide respiration. *Science* 346, 455–458. <https://doi.org/10.1126/science.1258118>
- Bosma, T.N.P., Middeldorp, P.J.M., Schraa, G., Zehnder, A.J.B., 1997. Mass transfer limitation of biotransformation: Quantifying bioavailability. *Environmental Science and Technology* 31, 248–252. <https://doi.org/10.1021/es960383u>
- Bullock, R.M., Che, J.G., Gagliardi, L., Chiri, P.J., Farh, O.K., Hendo, C.H., Jone, C.W., Keit, J.A., Klosin, J., Mintee, S.D., Morri, R.H., Radosevic, A.T., Rauchfus, T.B., Strotma, N.A.,

- Vojvodic, A., War, T.R., Yan, J.Y., Surendranath, Y., 2020. Using nature's blueprint to expand catalysis with Earth-abundant metals. *Science* 369, 786. <https://doi.org/10.1126/science.abc3183>
- Büsing, J., Buchner, D., Behrens, S., Haderlein, S.B., 2020. Deciphering the Variability of Stable Isotope (C, Cl) Fractionation of Tetrachloroethene Biotransformation by *Desulfitobacterium* strains Carrying Different Reductive Dehalogenases Enzymes. *Environmental Science and Technology* 54, 1593–1602. <https://doi.org/10.1021/acs.est.9b05606>
- Chan, C.C.H., Mundle, S.O.C., Eckert, T., Liang, X., Tang, S., Lacrampe-Couloume, G., Edwards, E.A., Sherwood Lollar, B., 2012. Large carbon isotope fractionation during biodegradation of chloroform by *Dehalobacter* cultures. *Environmental Science and Technology* 46, 10154–10160. <https://doi.org/10.1021/es3010317>
- Currin, A., Swainston, N., Day, P.J., Kell, D.B., 2015. Synthetic biology for the directed evolution of protein biocatalysts: Navigating sequence space intelligently. *Chemical Society Reviews* 44, 1172–1239. <https://doi.org/10.1039/c4cs00351a>
- Deshpande, N.P., Wong, Y.K., Manefield, M., Wilkins, M.R., Lee, M., 2013. Genome Sequence of *Dehalobacter* UNSWDHB, a Chloroform-Dechlorinating Bacterium 0–1. <https://doi.org/10.1186/1471-2105-11-485.7>
- Edgar, R.C., 2004. MUSCLE: Multiple sequence alignment with high accuracy and high throughput. *Nucleic Acids Research* 32, 1792–1797. <https://doi.org/10.1093/nar/gkh340>
- Edwards, E.A., Grbic-Galic, D., 1994. Anaerobic degradation of toluene and o-xylene by a methanogenic consortium. *Applied and Environmental Microbiology* 60, 313–322.
- Edwards, E.A., Grbić-Galić, D., 1992. Complete mineralization of benzene by aquifer microorganisms under strictly anaerobic conditions. *Applied and Environmental Microbiology* 58, 2663–2666.
- Ehrl, B.N., Gharasoo, M., Elsner, M., 2018. Isotope Fractionation Pinpoints Membrane Permeability as a Barrier to Atrazine Biodegradation in Gram-negative *Polaromonas* sp. Nea-C. *Environmental Science & Technology* 1–8. <https://doi.org/10.1021/acs.est.7b06599>

- Elizabeth Phillips, 2021. Use of Compound-Specific Isotope Analysis to Investigate Enzymatic Reaction Mechanisms. Toronto.
- Elsner, M., Zwank, L., Hunkeler, D., Schwarzenbach, R.P., 2005. A new concept linking observable stable isotope fractionation to transformation pathways of organic pollutants. *Environmental Science and Technology* 39, 6896–6916. <https://doi.org/10.1021/es0504587>
- Fent, K., 2003. Ecotoxicological problems associated with contaminated sites 141, 353–365. [https://doi.org/10.1016/S0378-4274\(03\)00032-8](https://doi.org/10.1016/S0378-4274(03)00032-8)
- Fincker, M., Spormann, A.M., 2017. Biochemistry of Catabolic Reductive Dehalogenation. *The Annual Review in Biochemistry* 86, 357–386. <https://doi.org/10.1146/annurev-biochem>
- Groster, A., Edwards, E.A., 2006. A 1,1,1-trichloroethane-degrading anaerobic mixed microbial culture enhances biotransformation of mixtures of chlorinated ethenes and ethanes. *Applied and Environmental Microbiology* 72, 7849–7856. <https://doi.org/10.1128/AEM.01269-06>
- Halliwell, T., Fisher, K., Payne, K.A.P., Rigby, S.E.J., Leys, D., 2021. Heterologous expression of cobalamin dependent class-III enzymes. *Protein Expression and Purification* 177. <https://doi.org/10.1016/j.pep.2020.105743>
- Health Canada, 2020. Guidelines for Canadian Drinking Water Quality Summary Table Health Canada Federal-Provincial-Territorial Committee on Drinking Water of the Federal-Provincial-Territorial Committee on Health and the Environment September 2020.
- Heckel, B., Cretnik, S., Kliegman, S., Shouakar-Stash, O., McNeill, K., Elsner, M., 2017. Reductive Outer-Sphere Single Electron Transfer Is an Exception Rather than the Rule in Natural and Engineered Chlorinated Ethene Dehalogenation. *Environmental Science and Technology* 51, 9663–9673. <https://doi.org/10.1021/acs.est.7b01447>
- Heckel, B., McNeill, K., Elsner, M., 2018. Chlorinated Ethene Reactivity with Vitamin B₁₂ Is Governed by Cobalamin Chloroethylcarbanions as Crossroads of Competing Pathways. *ACS Catalysis* 8, 3054–3066. <https://doi.org/10.1021/acscatal.7b02945>

Heckel, B., Phillips, E., Edwards, E., Sherwood Lollar, B., Elsner, M., Manefield, M.J., Lee, M., 2019. Reductive Dehalogenation of Trichloromethane by Two Different *Dehalobacter restrictus* Strains Reveal Opposing Dual Element Isotope Effects. *Environmental Science and Technology* 53, 2332–2343. <https://doi.org/10.1021/acs.est.8b03717>

Hug, L.A., Maphosa, F., Leys, D., Löffler, F.E., Smidt, H., Edwards, E.A., Adrian, L., 2013. Overview of organohalide-respiring bacteria and a proposal for a classification system for reductive dehalogenases. *Philosophical Transactions of the Royal Society B: Biological Sciences*. <https://doi.org/10.1098/rstb.2012.0322>

Hunkeler, D., Meckenstock, R.U., Sherwood Lollar, B., Schmidt, T.C., Wilson, J.T., 2008. A Guide for Assessing Biodegradation and Source Identification of Organic Ground Water Contaminants using Compound Specific Isotope Analysis (CSIA). USEPA Publication EPA 600/R-, 1–82. <https://doi.org/EPA/600/R-08/148>

Jiménez-Osés, G., Osuna, S., Gao, X., Sawaya, M.R., Gilson, L., Collier, S.J., Huisman, G.W., Yeates, T.O., Tang, Y., Houk, K.N., 2014. The Role of Distant Mutations and Allosteric Regulation on LovD Active Site Dynamics. *Nature Chemical Biology* 10, 431–436. <https://doi.org/10.1038/nchembio.1503>.The

Joint Committee for Guides in Metrology, 2008. Evaluation of Measurement Data - Part 3: Guide to the Expression of Uncertainty in Measurement.

Jugder, B.E., Bohl, S., Lebhar, H., Healey, R.D., Manefield, M., Marquis, C.P., Lee, M., 2017. A bacterial chloroform reductive dehalogenase: purification and biochemical characterization. *Microbial Biotechnology* 10, 1640–1648. <https://doi.org/10.1111/1751-7915.12745>

Jugder, B.E., Payne, K.A.P., Fisher, K., Bohl, S., Lebhar, H., Manefield, M., Lee, M., Leys, D., Marquis, C.P., 2018. Heterologous Production and Purification of a Functional Chloroform Reductive Dehalogenase. *ACS Chemical Biology* 13, 548–552. <https://doi.org/10.1021/acscchembio.7b00846>

Jumper, J., Evans, R., Pritzel, A., Green, T., Figurnov, M., Ronneberger, O., Tunyasuvunakool, K., Bates, R., Žídek, A., Potapenko, A., Bridgland, A., Meyer, C., Kohl, S.A.A., Ballard,

- A.J., Cowie, A., Romera-Paredes, B., Nikolov, S., Jain, R., Adler, J., Back, T., Petersen, S., Reiman, D., Clancy, E., Zielinski, M., Steinegger, M., Pacholska, M., Berghammer, T., Bodenstein, S., Silver, D., Vinyals, O., Senior, A.W., Kavukcuoglu, K., Kohli, P., Hassabis, D., 2021. Highly accurate protein structure prediction with AlphaFold. *Nature* 596, 583–589. <https://doi.org/10.1038/s41586-021-03819-2>
- Kim, D.E., Chivian, D., Baker, D., 2004. Protein structure prediction and analysis using the Robetta server. *Nucleic Acids Research* 32. <https://doi.org/10.1093/nar/gkh468>
- Kuntze, K., Eisenmann, H., Richnow, H.-H., Fischer, A., 2020. Compound-Specific Stable Isotope Analysis (CSIA) for Evaluating Degradation of Organic Pollutants: An Overview of Field Case Studies, in: *Anaerobic Utilization of Hydrocarbons, Oils, and Lipids*. pp. 1–39. https://doi.org/10.1007/978-3-319-33598-8_23-1
- Kunze, C., Bommer, M., Hagen, W.R., Uksa, M., Dobbek, H., Schubert, T., Diekert, G., 2017. Cobamide-mediated enzymatic reductive dehalogenation via long-range electron transfer. *Nature Communications* 8. <https://doi.org/10.1038/ncomms15858>
- Lee, M., Wells, E., Wong, Y.K., Koenig, J., Adrian, L., Richnow, H.H., Manefield, M., 2015. Relative contributions of *Dehalobacter* and zerovalent iron in the degradation of chlorinated methanes. *Environmental Science and Technology* 49, 4481–4489. <https://doi.org/10.1021/es5052364>
- Lihl, C., Douglas, L.M., Meyer, A.H., Franke, S., Pérez-de-Mora, A., Meyer, A.H., Daubmeier, M., Edwards, E.A., Nijenhuis, I., Sherwood Lollar, B., Elsner, M., 2019. Mechanistic Dichotomy in Bacterial Trichloroethene Dechlorination Revealed by Carbon and Chlorine Isotope Effects. *Environmental Science and Technology* 53, 4245–4254. <https://doi.org/10.1021/acs.est.8b06643>
- Mac Nelly, A., Kai, M., Svatoš, A., Diekert, G., Schubert, T., 2014. Functional heterologous production of reductive dehalogenases from *Desulfitobacterium hafniense* strains. *Applied and Environmental Microbiology* 80, 4313–4322. <https://doi.org/10.1128/AEM.00881-14>

- Mancini, S.A., Hirschorn, S.K., Elsner, M., Lacrampe-Couloume, G., Sleep, B.E., Edwards, E.A., Sherwood Lollar, B., 2006. Effects of trace element concentration on enzyme controlled stable isotope fractionation during aerobic biodegradation of toluene. *Environmental Science and Technology* 40, 7675–7681. <https://doi.org/10.1021/es061363n>
- Marcus A., R., 1992. Electron Transfer Reactions in Chemistry: Theory and Experiment (Nobel Lecture), in: *Angewandte Chemie International Edition in English*. pp. 1111–1121.
- Mariotti, A., Germon, J.C., Hubert, P., Kaiser, P., Letolle, R., Tardieux, A., Tardieux, P., 1981. Experimental determination of nitrogen kinetic isotope fractionation: Some principles; illustration for the denitrification and nitrification processes. *Plant and Soil* 62, 413–430. <https://doi.org/10.1007/BF02374138>
- Michaelis, L., Menten, M.L., 1913. Die Kinetik der Invertinwirkung. *Biochem Z* 49, 333–369. <https://doi.org/10.1021/bi201284u>
- Molenda, O., Puentes Jácome, L.A., Cao, X., Nesbø, C.L., Tang, S., Morson, N., Patron, J., Lomheim, L., Wishart, D.S., Edwards, E.A., 2020. Insights into origins and function of the unexplored majority of the reductive dehalogenase gene family as a result of genome assembly and ortholog group classification. *Environmental Science: Processes and Impacts* 22, 663–678. <https://doi.org/10.1039/c9em00605b>
- Morley, K.L., Kazlauskas, R.J., 2005. Improving enzyme properties: When are closer mutations better? *Trends in Biotechnology* 23, 231–237. <https://doi.org/10.1016/j.tibtech.2005.03.005>
- Murdoch, R.W., Chen, G., Murdoch, F.K., Mack, E.E., Villalobos Solis, M.I., Hettich, R.L., Löffler, F.E., 2021. Global distribution of anaerobic dichloromethane degradation potential. *Classification: Biological Sciences (Major); Environmental Sciences*. <https://doi.org/10.1101/2021.08.30.458270>
- Nakamura, R., Obata, T., Nojima, R., Hashimoto, Y., Noguchi, K., Ogawa, T., Yohda, M., 2018. Functional expression and characterization of tetrachloroethene dehalogenase from *Geobacter* sp. *Frontiers in Microbiology* 9, 1–7. <https://doi.org/10.3389/fmicb.2018.01774>

National Institute of Standards and Technology (NIST), 2019. Good Laboratory Practice for Rounding Expanded Uncertainties and Calibration Values. Gaithersburg, MD.

<https://doi.org/10.6028/NIST.IR.6969-2019>

Nijenhuis, I., Andert, J., Beck, K., Kästner, M., Diekert, G., Richnow, H.H., 2005. Stable isotope fractionation of tetrachloroethene during reductive dechlorination by *Sulfurospirillum multivorans* and *Desulfitobacterium* sp. strain PCE-S and abiotic reactions with cyanocobalamin. *Applied and Environmental Microbiology* 71, 3413–3419.

<https://doi.org/10.1128/AEM.71.7.3413-3419.2005>

Northrop, D.B., 1981. The expression of isotope effects on enzyme-catalyzed reactions. *Annual Review of Biochemistry* 50, 103–131. <https://doi.org/10.1146/annurev.bi.50.070181.000535>

Ojeda, A.S., Phillips, E., Mancini, S.A., Sherwood Lollar, B., 2019. Sources of uncertainty in biotransformation mechanistic interpretations and remediation studies using CSIA. *Analytical Chemistry* 91, 9147–9153.

Ojeda, A.S., Phillips, E., Sherwood Lollar, B., 2020. Multi-element (C, H, Cl, Br) stable isotope fractionation as a tool to investigate transformation processes for halogenated hydrocarbons. *Environmental Science: Processes & Impacts*. <https://doi.org/10.1039/c9em00498j>

O’Leary, M.H., 1989. Multiple isotope effects on enzyme-catalyzed reactions. *Annual Reviews in Biochemistry*.

Paramesvaran, J., Hibbert, E.G., Russell, A.J., Dalby, P.A., 2009. Distributions of enzyme residues yielding mutants with improved substrate specificities from two different directed evolution strategies. *Protein Engineering, Design and Selection* 22, 401–411.

<https://doi.org/10.1093/protein/gzp020>

Parthasarathy, A., Stich, T.A., Lohner, S.T., Lesnefsky, A., Britt, R.D., Spormann, A.M., 2015. Biochemical and EPR-Spectroscopic Investigation into Heterologously Expressed Vinyl Chloride Reductive Dehalogenase (VcrA) from *Dehalococcoides mccartyi* Strain VS.

Journal of the American Chemical Society 137, 3525–3532.

<https://doi.org/10.1021/ja511653d>

Payne, K.A.P., Quezada, C.P., Fisher, K., Dunstan, M.S., Collins, F.A., Sjuts, H., Levy, C., Hay, S., Rigby, S.E.J., Leys, D., 2015. Reductive dehalogenase structure suggests a mechanism for B₁₂-dependent dehalogenation. *Nature* 517, 513–516.

<https://doi.org/10.1038/nature13901>

Picott, K.J., Flick, R., Edwards, E.A., 2022. Heterologous Expression of Active *Dehalobacter* Respiratory Reductive Dehalogenases in *Escherichia coli*. *Applied and Environmental Microbiology* 88, 1–16.

Renpenning, J., Horst, A., Schmidt, M., Gehre, M., 2018. Online isotope analysis of ³⁷Cl/³⁵Cl universally applied for semi-volatile organic compounds using GC-MC-ICPMS. *Journal of Analytical Atomic Spectrometry* 33, 314–321. <https://doi.org/10.1039/c7ja00404d>

Renpenning, J., Keller, S., Cretnik, S., Shouakar-Stash, O., Elsner, M., Schubert, T., Nijenhuis, I., 2014. Combined C and Cl isotope effects indicate differences between corrinoids and enzyme (*Sulfurospirillum multivorans* PceA) in reductive dehalogenation of tetrachloroethene, but not trichloroethene. *Environmental Science and Technology* 48, 11837–11845. <https://doi.org/10.1021/es503306g>

Renpenning, J., L. Hitzfeld, K., Gilevska, T., Nijenhuis, I., Gehre, M., Richnow, H.-H., 2015a. Development and Validation of an Universal Interface for Compound-Specific Stable Isotope Analysis of Chlorine (³⁷Cl/³⁵Cl) by GC-High-Temperature Conversion (HTC)-MS/IRMS. *Analytical Chemistry* 87, 2832–2839. <https://doi.org/10.1021/ac504232u>

Renpenning, J., Rapp, I., Nijenhuis, I., 2015b. Substrate Hydrophobicity and Cell Composition Influence the Extent of Rate Limitation and Masking of Isotope Fractionation during Microbial Reductive Dehalogenation of Chlorinated Ethenes. *Environmental Science and Technology* 49, 4293–4301. <https://doi.org/10.1021/es506108j>

Rodríguez-Fernández, D., Heckel, B., Torrentó, C., Meyer, A., Elsner, M., Hunkeler, D., Soler, A., Rosell, M., Domènech, C., 2018. Dual element (C-Cl) isotope approach to distinguish abiotic reactions of chlorinated methanes by Fe(0) and by Fe(II) on iron minerals at neutral and alkaline pH. *Chemosphere* 206, 447–456.

<https://doi.org/10.1016/j.chemosphere.2018.05.036>

- Rowe, B.L., Toccalino, P.L., Moran, M.J., Zogorski, J.S., Price, C. v., 2007. Occurrence and potential human-health relevance of volatile organic compounds in drinking water from domestic wells in the United States. *Environmental Health Perspectives* 115, 1539–1546. <https://doi.org/10.1289/ehp.10253>
- Saveant, J.M., 1990. Single Electron Transfer and Nucleophilic Substitution, in: Bethell, D. (Ed.), *Advances in Physical Organic Chemistry*. Academic Press, pp. 1–130.
- Schmitz, R.P.H., Wolf, J., Habel, A., Neumann, A., Ploss, K., Svatos, A., Boland, W., Diekert, G., 2007. Evidence for a radical mechanism of the dechlorination of chlorinated propenes mediated by the tetrachloroethene reductive dehalogenase of *Sulfurospirillum multivorans*. *Environmental Science and Technology* 41, 7370–7375. <https://doi.org/10.1021/es071026u>
- Schrauzer, G.N., Deutsch, E., 1968. Reactions of Cobalt(I) Supernucleophiles. The Alkylation of Vitamin B₁₂S, Cobaloximes(I) and Related Compounds. *Journal of the American Chemical Society* 91, 3341–3350.
- Schrödinger LLC, 2021. The PyMOL Molecular Graphics System.
- Sherwood Lollar, B., Hirschorn, S., Mundle, S.O.C., Grostern, A., Edwards, E.A., Lacrampe-Couloume, G., 2010. Insights into enzyme kinetics of chloroethane biodegradation using compound specific stable isotopes. *Environmental Science and Technology* 44, 7498–7503. <https://doi.org/10.1021/es101330r>
- Sherwood Lollar, B., Hirschorn, S.K., Chartrand, M.M.G., Lacrampe-Couloume, G., 2007. An approach for assessing total instrumental uncertainty in compound-specific carbon isotope analysis: implications for environmental remediation studies. *Analytical Chemistry* 79, 3469–3475. <https://doi.org/10.1021/ac062299v>
- Soder-Walz, J.M., Torrentó, C., Algora, C., Wasmund, K., Cortés, P., Soler, A., Vicent, T., Rosell, M., Marco-Urrea, E., 2022. Trichloromethane dechlorination by a novel *Dehalobacter* sp. strain 8M reveals a third contrasting C and Cl isotope fractionation pattern within this genus. *Science of the Total Environment* 813. <https://doi.org/10.1016/j.scitotenv.2021.152659>

Świderek, K., Paneth, P., 2013. Binding isotope effects. Chemical Reviews.

<https://doi.org/10.1021/cr300515x>

Tang, S., Edwards, E.A., 2013. Identification of *Dehalobacter* reductive dehalogenases that catalyse dechlorination of chloroform, 1,1,1-trichloroethane and 1,1-dichloroethane.

Philosophical Transactions of the Royal Society B: Biological Sciences 368.

<https://doi.org/10.1098/rstb.2012.0318>

Tang, S., Gong, Y., Edwards, E.A., 2012. Semi-Automatic In Silico Gap Closure Enabled De Novo Assembly of Two *Dehalobacter* Genomes from Metagenomic Data. PLoS ONE 7.

<https://doi.org/10.1371/journal.pone.0052038>

Thullner, M., Fischer, A., Richnow, H., Wick, L.Y., 2013. Influence of mass transfer on stable isotope fractionation. Applied Microbiology and Biotechnology 441–452.

<https://doi.org/10.1007/s00253-012-4537-7>

USEPA (United States Environmental Protection Agency), 2012. Drinking water standards and health advisories. Washington DC, U.S.A., EPA 822-S-12-001.

Vogt, C., Dorer, C., Musat, F., Richnow, H.H., 2016. Multi-element isotope fractionation concepts to characterize the biodegradation of hydrocarbons - from enzymes to the environment. Current Opinion in Biotechnology.

<https://doi.org/10.1016/j.copbio.2016.04.027>

Wang, H., Yu, R., Webb, J., Dollar, P., Freedman, D.L., 2022. Anaerobic Biodegradation of Chloroform and Dichloromethane with a *Dehalobacter* Enrichment Culture. Applied and Environmental Microbiology 88.

Wang, P.H., Tang, S., Nemr, K., Flick, R., Yan, J., Mahadevan, R., F Yakunin, A., Löffler, F.E., Edwards, E.A., 2017. Refined experimental annotation reveals conserved corrinoid autotrophy in chloroform-respiring *Dehalobacter* isolates. ISME Journal 11, 626–640.

<https://doi.org/10.1038/ismej.2016.158>

Ward, J.A., Slater, G.F., Moser, D.P., Lin, L.H., Lacrampe-Couloume, G., Bonin, A.S.,

Davidson, M., Hall, J.A., Mislowack, B., Bellamy, R.E.S., Onstott, T.C., Sherwood Lollar,

- B., 2004. Microbial hydrocarbon gases in the Witwatersrand Basin, South Africa: Implications for the deep biosphere. *Geochimica et Cosmochimica Acta* 68, 3239–3250. <https://doi.org/10.1016/j.gca.2004.02.020>
- Williams, C.J., Headd, J.J., Moriarty, N.W., Prisant, M.G., Videau, L.L., Deis, L.N., Verma, V., Keedy, D.A., Hintze, B.J., Chen, V.B., Jain, S., Lewis, S.M., Arendall, W.B., Snoeyink, J., Adams, P.D., Lovell, S.C., Richardson, J.S., Richardson, D.C., 2018. MolProbity: More and better reference data for improved all-atom structure validation. *Protein Science* 27, 293–315. <https://doi.org/10.1002/pro.3330>
- Wong, Y.K., Holland, S.I., Ertan, H., Manefield, M., Lee, M., 2016. Isolation and characterization of *Dehalobacter sp.* strain UNSWDHB capable of chloroform and chlorinated ethane respiration. *Environmental Microbiology* 18, 3092–3105. <https://doi.org/10.1111/1462-2920.13287>
- World Health Organization, 2004. EHC 216: Disinfectants and Disinfectant By-products, Environmental Health Criteria.
- Ye, L., Schilhabel, A., Bartram, S., Boland, W., Diekert, G., 2010. Reductive dehalogenation of brominated ethenes by *Sulfurospirillum multivorans* and *Desulfitobacterium hafniense* PCE-S. *Environmental Microbiology* 12, 501–509. <https://doi.org/10.1111/j.1462-2920.2009.02093.x>
- York, D., Evensen, N.M., Martínez, M.L., de Basabe Delgado, J., 2004. Unified equations for the slope, intercept, and standard errors of the best straight line. *American Journal of Physics* 72, 367–375. <https://doi.org/10.1119/1.1632486>
- Zhao, S., Ding, C., He, J., 2015. Detoxification of 1,1,2-trichloroethane to ethene by *Desulfitobacterium* and identification of its functional reductase gene. *PLoS ONE* 10, 1–13. <https://doi.org/10.1371/journal.pone.0119507>
- Zhao, S., Rogers, M.J., He, J., 2017. Microbial reductive dehalogenation of trihalomethanes by a *Dehalobacter*-containing co-culture. *Applied Microbiology and Biotechnology* 101, 5481–5492. <https://doi.org/10.1007/s00253-017-8236-2>

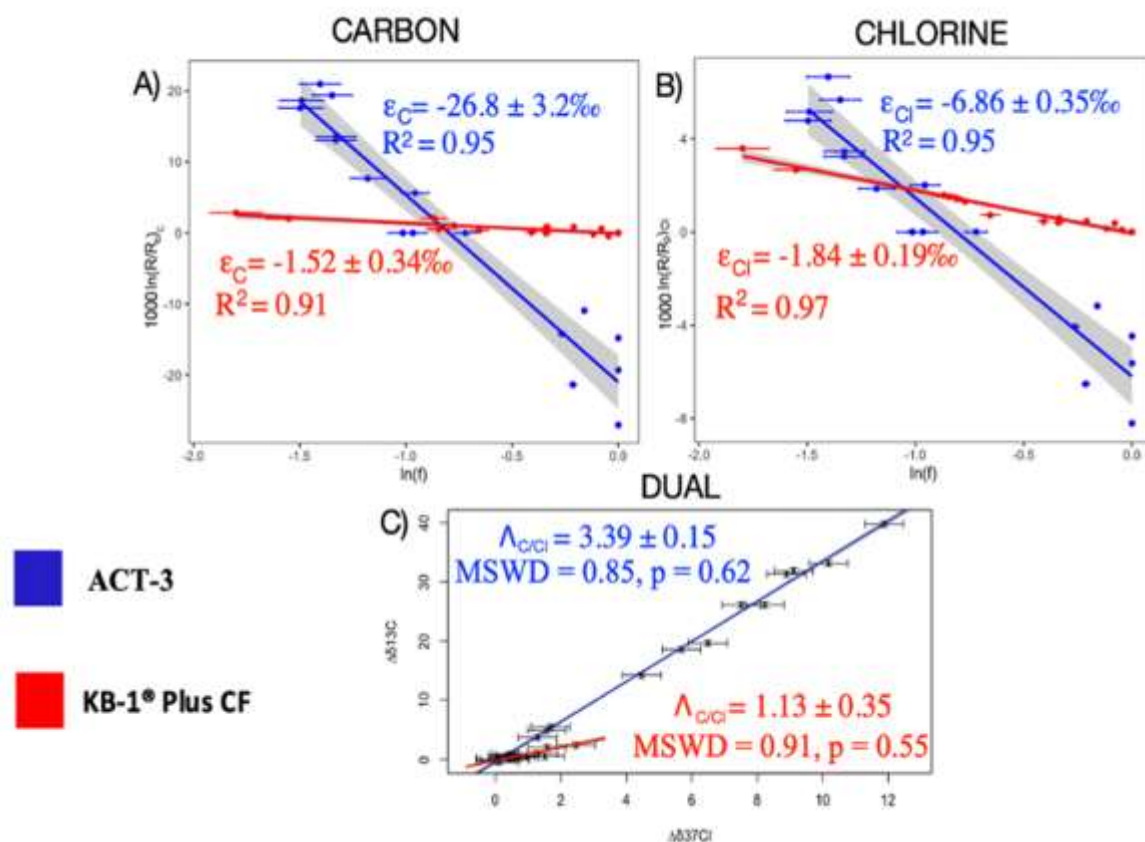


Figure 1. Rayleigh plots for carbon (A), and chlorine (B) and dual plot (C) for CF degradation by ACT-3 (blue) and KB-1® Plus CF (red). Error bars on the Rayleigh plots represent propagated uncertainty of concentrations (x-axes) and isotope measurements (y-axes). Dual-plots were regressed using the York method (York et al., 2004) as recommended by Ojeda et al. (2019). Mean square of weighted deviates (MSWD) and the associated p-value from York regression output were used to assess model fit (see detailed discussion in Ojeda et al., 2021). Error bars on the dual-plots represent analytical uncertainty for each element. Uncertainty of ϵ and Λ is calculated as 95% C.I. of the slope. Shading around the best fit line shows 95% confidence interval of the slope.

ORIGINAL UNPUBLISHED

		KB-1® Plus CF						
		CfrA	RdhA	DcrA	TmrA	CtrA	ThmA	
KB-1® Plus CF	CfrA		19	23	21	28	21	Number of AA Differences
	RdhA	95.8%		15	15	29	21	
	DcrA	95.0%	96.7%		22	28	20	
	TmrA	95.4%	96.7%	95.2%		27	19	
	CtrA	93.9%	93.7%	93.9%	94.1%		10	
	ThmA	95.4%	95.4%	95.6%	95.8%	97.8%		
		Percent Identity						

Figure 2. Matrix showing differences in amino acid sequences between RDases in OG97. The number of amino acids differing between protein sequences is shown in upper part of table (shaded in green) out of a total of 456 amino acids. Percent identity (the number of identical residues in the same location in an amino acid alignment) is shown lower part of table (shaded in grey).

AA position	78	257	386
KB-1® Plus CF RdhA	NIFGQ	GLSYAQIGY	KCFEFWSR
CfrA	NIYQ*	GLSCAQIGY	KCLEFMSR
TmrA	NIFGQ	GLSFAQIGY	KCFEFWSR
DcrA	NIWGQ	GLSYTQIGY	KCFEFWSR
CtrA	NIFGQ	GLGCAQYGY	KCLEFWSR
ThmA	NIFGQ	GLSCAQYGY	KCLEFWSR

Figure 3. Alignment of key active site residues for chlorinated alkane RDases in OG 97. RDases without isotope data are indicated by grey text (ThmA, CtrA). Coloured residues indicate where key residues differ from the consensus sequence, and stars mark residues that differ between CfrA and the KB-1® Plus CF RdhA (sequence in S.I.). Alignments were created using published sequences for ThmA (Accession No.: ANI21407), CtrA (AGO27983), TmrA (WP_034377773), CfrA (AFV05253), and DcrA (WP_015043247); (Deshpande et al., 2013; Tang et al., 2012; Zhao et al., 2017, 2015).

ACT-3/CF CfrA
Unique Residues
Iron-sulfur clusters
Cobalamin

KB-1® Plus CF RdhA
Unique Residues
Iron-sulfur clusters
Cobalamin

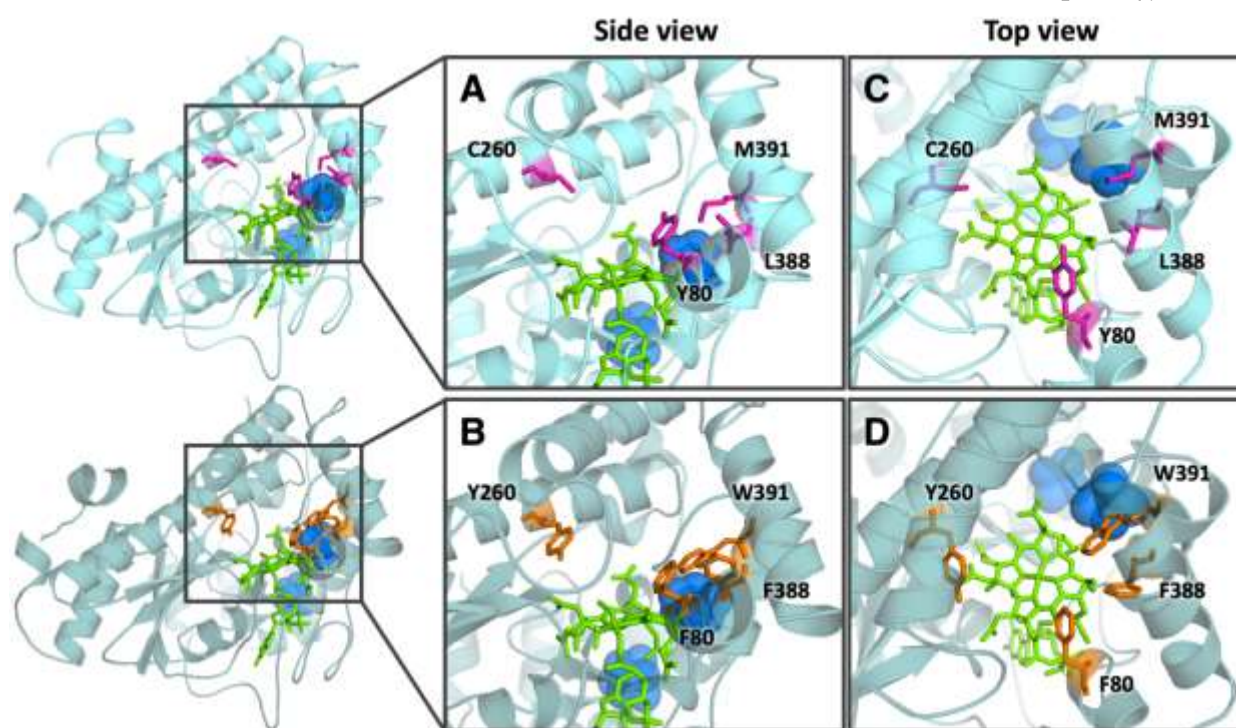


Figure 4. Models of the reductive dehalogenases in ACT-3/CF (A, C) and KB-1® Plus CF (B, D) from a side view (A, B) and top view (C, D). Amino acid residues unique to CfrA are shown in pink (A, C), and in the KB-1® Plus CF RdhA are shown in orange (B, D). The active site includes cobalamin (shown in green). The [4Fe-4S] clusters (blue) and cobalamin are superimposed from the reference RDase structure (NpRdhA (Kunze et al., 2017)).

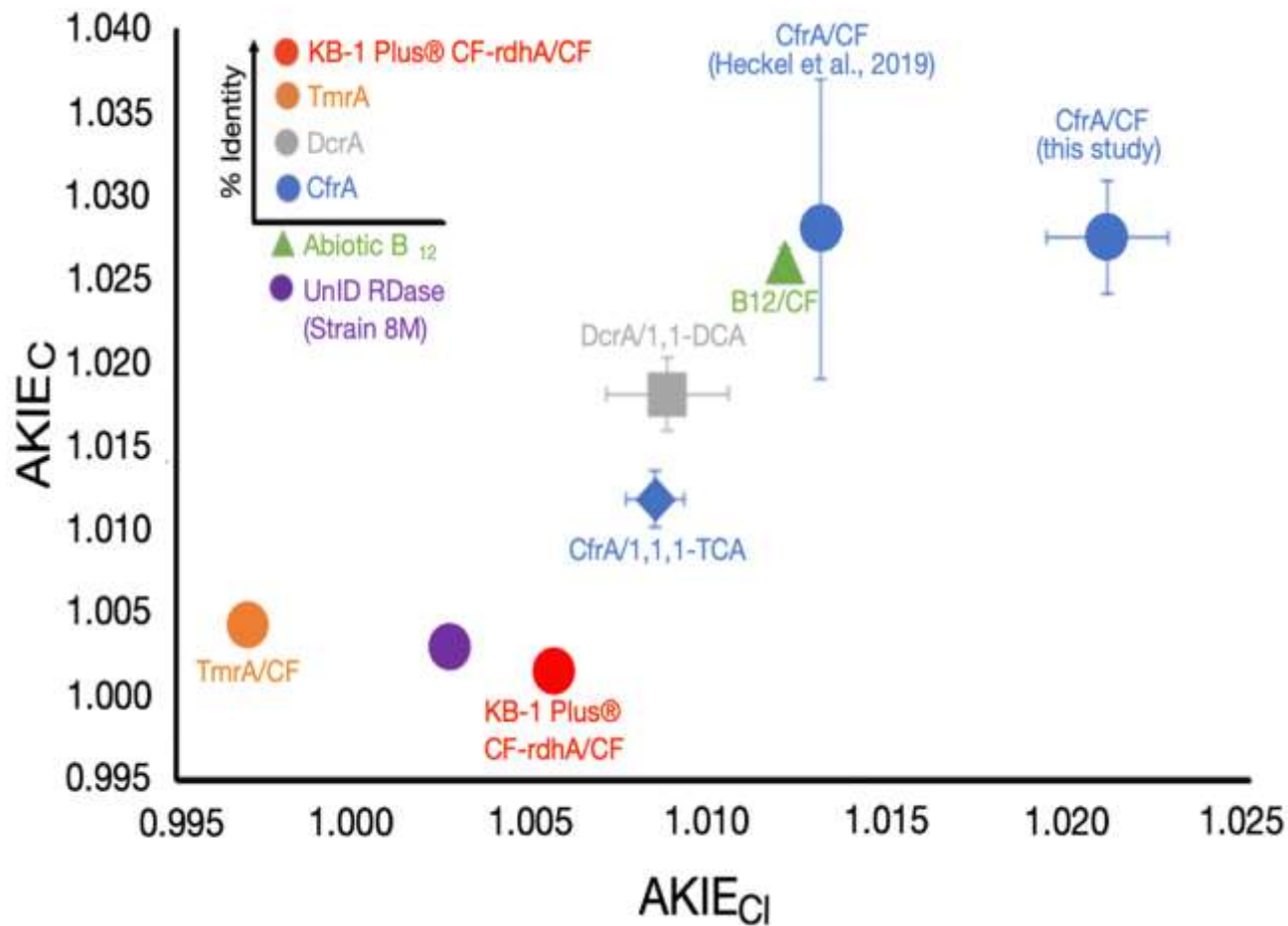


Figure 5. Carbon vs. chlorine AKIE values for substrates shown for different reductive dehalogenases in OG 97 (unpublished data from Philips, 2021 for 1,1-DCA (DcrA enzyme) and 1,1,1-TCA (same CfrA enzyme as shown in Table 1). Each point is annotated showing RDase name/substrate. The green diamond shows abiotic cobalamin (Vitamin B₁₂, as shown in Table 1). For Strain 8M (Soder-Walz et al., 2022), the enzyme responsible for CF transformation is unnamed/uncharacterized (shown as UnID/strain 8M in figure). Increasing % identity in relation to KB-1® Plus CF RdhA is shown by the black arrow next to the legend based on the similarity matrix shown in Figure 2. Where not visible, error bars are smaller than plotted symbols.

Table 1. Published carbon apparent kinetic isotope effects (AKIE_C) and chlorine (AKIE_{Cl}) for CF (bio)transformation from this work and the literature. Isotope data are presented for CfrA (This work; Chan et al., 2012; Heckel et al., 2019), abiotic cyanocobalamin (Heckel et al., 2019), KB-1® Plus CF -rdhA (This work), TmrA (Heckel et al., 2019), and *Dhb* strain 8M (RDase has not been identified; Soder-Walz et al., 2022). Lines are color coded for high degree of C and Cl fractionation (shaded green) and low degree (shaded orange). Footnotes at bottom of table show the variety of substrates each RDase has been shown to date to be able to biodegrade. NA – no data available in literature to date to our knowledge.

Culture Name	Strain (microbe)	Enzyme	Study	ϵ_C	AKIE_C	ϵ_{Cl} (Instrument)	AKIE_{Cl}	$\Lambda_{C/Cl}$
ACT-3	<i>Dhb</i> strain CF	CfrA	This work (Phillips et al.)	$-26.8 \pm 3.2\%$	1.0275 ± 0.0034	$-6.86 \pm 0.35\%$ (MC-ICP-MS)	1.02101 ± 0.00012	3.39 ± 0.15
			Heckel et al., 2019	$-27.91 \pm 1.66\%$	1.028 ± 0.009	$-4.20 \pm 0.26\%$ (IRMS)	1.013 ± 0.0002	6.64 ± 0.14
			Chan et al., 2012	$-27.5 \pm 0.9\%$	1.028 ± 0.002	NA	NA	NA

ORIGINAL UI

Abiotic cyanocobalamin	NA	NA	Heckel et al., 2019	-26.04 ± 0.91‰	1.026 ± 0.0009	-4.00 ± 0.20‰	1.012 ± 0.0002	6.46 ± 0.20
KB-1® Plus CF	<i>Dhb</i> (not named)	KB-1® Plus CF - RdhA	This work (Phillips et al.)	-1.52 ± 0.34‰	1.00152 ± 0.00034	-1.84 ± 0.19‰	1.005551 ± 0.000036	1.13 ± 0.35
CFH2	<i>Dhb</i> strain UNSWDHB	TmrA	Heckel et al., 2019	-3.1 ± 0.5‰	1.003 ± 0.0005	2.5 ± 0.3‰	0.997 ± 0.0003	-1.2 ± 0.2
			Lee et al., 2015	-4.3 ± 0.45‰	1.004 ± 0.00045	NA	NA	NA
Enrich. culture (not named)	<i>Dhb</i> strain 8M	Not identified	Soder-Walz et al., 2022	-2.8 ± 0.2‰	1.0028 ± 0.0002	-0.9 ± 0.2‰ (qMS)	1.0027 ± 0.0002	2.8 ± 0.5

CfrA = CF, 1,1,1-TCA, 1,1,2-TCA

CtrA = CF, 1,1,1-TCA, 1,1,2-TCA (no CF biotransformation isotope data)

KB-1® Plus CF-RdhA = CF, 1,1,1-TCA

ThmA = CF, 1,1,1-TCA, Bromoform (no CF biotransformation isotope data)

TmrA = CF, 1,1,1-TCA, Vinyl Bromide

ORIGIN